

EXPLORING THE DISTRIBUTION AND NATURE OF SHOCK DEFORMATION IN AN ENSTATITE CHONDRULE AT SUBMICRON RESOLUTION BY A COMBINATION OF CL, ELECTRON BACKSCATTER DIFFRACTION, EDS MAPPING AND EPMA

M. R. M. Izawa^{1*}, D. E. Moser¹, I. R. Barker¹, R. L. Flemming¹, Z. Gainsforth², J. Stodolna², S. Matveev³, N. R. Banerjee¹

¹Dept. Earth Sciences, The University of Western Ontario, 1151 Richmond St., London, ON, Canada N6A5B7; ²Space Sciences Laboratory, Berkeley University 7 Gauss Way, Berkeley, CA 94720, USA; ³Dept. Earth and Atmospheric Sciences, University of Alberta, Edmonton, AB, Canada T6G 2E3
*matthew.izawa@gmail.com

Introduction: Shock metamorphic effects are ubiquitous in planetary materials. Constraining meteorite petrogenesis therefore requires that shock metamorphism be understood, both for its own sake, and to better perceive non-shock textures preserved in early solar system materials. Previous studies [e.g., 1,2] have demonstrated an effect of shock metamorphism on X-ray diffraction (XRD). This was interpreted as resulting from the progressive formation of shock-induced misoriented lattice domains with increased peak shock pressure however the distribution of strain was not resolvable [2]. Numerous studies using TEM have shown that shock-deformed enstatite contains abundant nanoscale structures, most notably lamellar intergrowths of clinoenstatite and orthoenstatite due to shearing at the unit-cell level. Because similar ortho-clino intergrowths can also result from quenching, other criteria such as a heterogeneous distribution of lamellae are required to assign a shock origin [3 and references therein]. Here, we report further explore the nature of shock-induced strain in a single porphyritic pyroxene chondrule with electron backscatter diffraction (EBSD) strain and phase ID mapping supported by cathodoluminescence (CL) and energy-dispersive X-ray spectroscopy (EDS) mapping. The chondrule is hosted within the EH4 chondrite MET 00783, previously classified as shock stage S4 [2]. The results shed new light on shock microdeformation in enstatite chondrites.

Materials and methods: A petrographic thin section was polished for EBSD using colloidal alumina, this step is necessary to produce a sufficiently flat and undamaged surface layer so that diffracted electrons could be detected. The sections were coated with a thin (~5 nm) layer of Os, and studied using a Hitachi SU6600 Field Emission SEM (FESEM) equipped with a Gatan Chroma-CL detector, Oxford Instruments INCA EDS system. Compositions of enstatite, plagioclase, kamacite, and troilite were measured using a JEOL8900R electron microprobe (EPMA).

Results and Discussion: *Enstatite:* Figure 1 shows BSE and CL images of the MET 00783 chondrule. The chondrule is dominated by near end-member enstatite. Mapping by EBSD reveals an apparently random fabric within chondrule (Fig. 2). Detailed EBSD mapping (step size 800 nm) reveals a weak lamellar fabric corresponding to subtle

differences in Kikuchi band contrast. The lamellar features are also revealed in CL imagery as subtle differences in CL emission intensity. The lamellar substructures are not related to elemental differences detectable by EDS or EPMA (Table 1). The average misorientation within the lamellar-textured grains is ~1.0-2.0°, measured over ~10 µm long profiles, which is above the misorientation detection limit of ~0.5°. Further investigation will determine whether this corresponds to the asterism observed in micro-XRD [2]. Similar degrees of misorientation are observed in some enstatite grains external to the chondrule, indicating that these microstructures are pervasive. Because grains both external and internal to the chondrule contain similar substructures, we interpret the substructures as the result of asteroidal rather than nebular processes.

Alkali-aluminosilicate (diaplectic?) glasses: Areas of Na- and Al-rich material detected by EDS mapping and EPMA are conspicuous as red areas in CL imagery (Fig. 1B). EBSD of these areas reveals no diffraction patterns, indicating that these are likely amorphous feldspathic glasses. The glasses occur in elongate domains interstitial to enstatite crystals, and appear to be parallel to enstatite crystal margins. Based on previous experience with EH4 chondrites, primary mesostasis glasses are commonly recrystallized and therefore our working interpretation is that the glassy feldspathic material observed is maskelynite (diaplectic feldspar glass formed via shock).

Conclusions: Preliminary EBSD results indicate that heterogeneously-distributed lamellar substructures are detectable within shocked enstatite grains. EBSD strain and orientation measurements may provide a link between macro-scale mosaicity detected by optical microscopy, asterism in micro-XRD diffraction patterns, and nanoscale structures due to unit-cell scale shock metamorphic changes.

References: [1] F. Hörz & W. L. Quaide 1973 *The Moon* 6: 45-86; [2] M. R. M. Izawa et al., 2011 *MAPS* 46(5):638-651; [3] H. Leroux *Eur. J. Mineral.* 2001, 13, 253-272

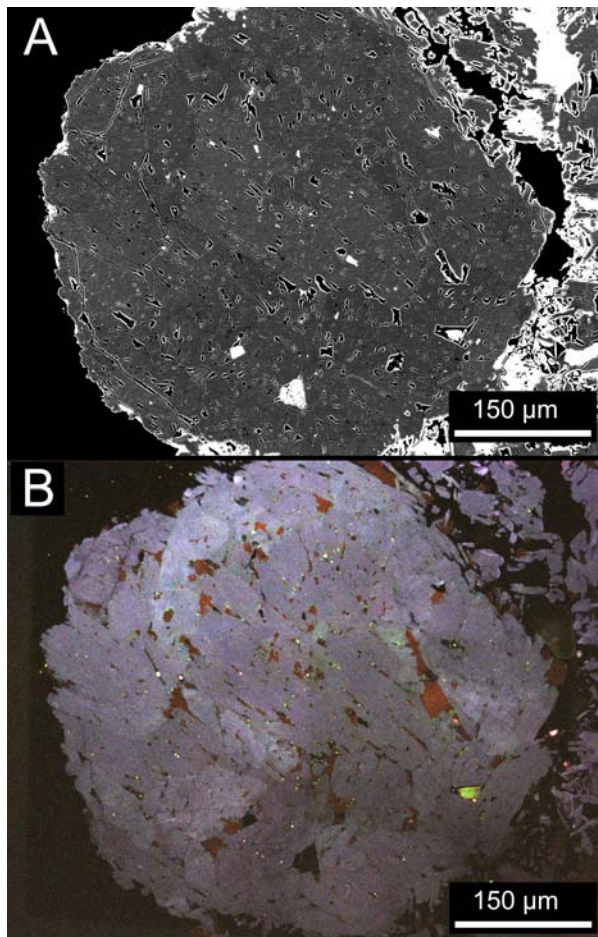


Figure 1: The MET 00783 chondrule investigated in this study is a porphyritic pyroxene chondrule dominated by enstatite with interstitial feldspathic mesostasis and minor troilite and Fe-Ni metal. A) SEM-BSE image and B) SEM-CL image. Blue luminescent grains are enstatite; red areas are plagioclase-composition mesostasis.

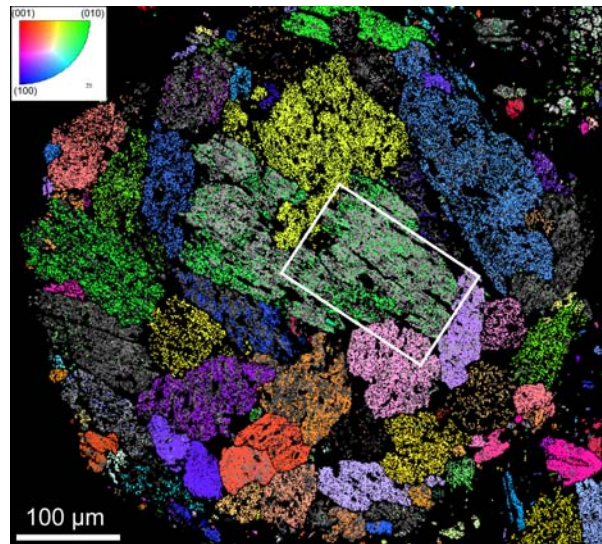


Figure 2: EBSD Inverse Pole Figure (IPF) map for orthoenstatite at 800 nm step size overlaid on a band contrast image of the MET 00783 chondrule in petrographic thin section. Colours correspond to crystallographic orientation normal to the sample surface. This figure illustrates the apparently random crystallographic orientations of grains and subgrains in the chondrule as well as a weak lamellar fabric corresponding to variations in diffraction pattern quality (e.g. box). Black domains within the chondrule are non-diffracting mesostasis, or holes/pluck marks in the thin section (distinguishable by comparison with Fig. 1).

Table 1: Summary of EPMA analysis for MET 00783 enstatite, feldspathic glass, troilite and Fe-Ni metal.

	TiO ₂	Al ₂ O ₃	Cr ₂ O ₃	FeO	MnO	MgO	CaO	Na ₂ O	K ₂ O		total		
Enstatite	59.6	b.d.	0.4	b.d.	0.6	b.d.	38.8	b.d.	b.d.		99.6		
Feldspathic glass	69.7	b.d.	18.6	b.d.	0.2	b.d.	0.3	0.6	9.9		100.3		
	Fe	Mg	Ca	Ti	Cr	Mn	Co	Ni	Cu	Zn	Si	S	total
Troilite	61.0	b.d.	b.d.	0.4	0.3	b.d.	b.d.	b.d.	b.d.	b.d.	b.d.	36.3	98.2
	Fe	Ni	Si	Cr	Co	S						total	
Fe-Ni metal	91.4	3.6	2.9	b.d.	0.6	b.d.						98.5	

b.d. = below detection (~0.02 wt%) F, Cl below detection in silicates. Number of analyses: enstatite n=10, feldspathic glass n=1, troilite n=3, Fe-Ni metal n=3.